Arch. Pharm. Chem. Life Sci. 2016, *349*, 327–341

ARCH PHARM
Archiv der Pharmazie

Full Paper

New Hydroxyquinoline-Based Derivatives as Potent Modulators of Amyloid-β Aggregations

Chin-Lan Fu[1], Li-Shin Hsu[1], Yung-Feng Liao[2], and Ming-Kuan Hu[1]

[1] School of Pharmacy, National Defense Medical Center, Taipei, Taiwan
[2] Laboratories of Molecular Neurobiology, Institute of Cellular and Organismic Biology, Academia Sinica, Taipei, Taiwan

Copper and zinc have been found to contribute to the burden of amyloid-β (Aβ) aggregations in neurodegenerative Alzheimer's disease (AD). Dysregulation of these metals leads to the generation of reactive oxygen species (ROS) and eventually results in oxidative damage and accumulation of the Aβ peptide, which are the key elements of the disease. Aiming to pursue the discovery of new modulators for the disease, we here rationally focused on conjugating the core hydroxyquinoline of the metal-protein attenuating compound PBT2 and the *N*-methylanilide analogous moiety of the Aβ imaging agent to build a new type of multi-target modulators of Aβ aggregations. We found that the *N*,*N*-dimethylanilinyl imines **7a**, **8a**, and the corresponding amines **7b**, **8b** exerted efficient inhibition of Cu^{2+}- or Zn^{2+}-induced Aβ aggregations and significant disassembly of metal-mediated Aβ aggregated fibrils. Further, **7a** and **7b** also exhibited significant ROC scavenging effects compared to PBT2. The results suggested that **7a** and **7b** are promising lead compounds for the development of a new therapy for AD.

Keywords: Alzheimer's disease / Amyloid-β aggregations / Multi-target modulators / Reactive oxygen species

Received: December 18, 2015; Revised: February 16, 2016; Accepted: February 23, 2016

DOI 10.1002/ardp.201500453

Introduction

Alzheimer's disease (AD) is characterized as a progressively neurodegenerative disorder with the extracellular senile plaques and intracellular neurofibrillary tangles (NFTs) as the hallmarks in the brain [1, 2]. The senile plaques are deposits of the various amyloid-β (Aβ) aggregates and the neurofibrillary tangles are mainly derived from hyperphosphorylated τ proteins under pathological conditions. Both Aβ aggregates and hyperphosphorylated τ together exert their effects on depriving axonal transport, resulting in neuronal damage and degeneration [3, 4]. Although the formation of Aβ aggregates is not fully elucidated, much evidence in recent decades has indicated that the aggregation of Aβ is closely involved in the disruption of metal ions homeostasis in the brain neurons; especially the physiological dysregulation of copper is known to facilitate Aβ assemblies by binding to the Aβ peptide [5, 6]. This interaction promotes the generation of copper-dependent amyloid oligomers, which contribute to Aβ toxicity through secretory pathways. In particular, these amyloid oligomers intracellularly and extracellularly downstream engaged certain proteins in the Aβ toxicities, including the receptor tyrosine kinase EphB2 and the receptor for advanced glycation end products [7, 8]. These effects eventually resulted in synaptic dysfunction and memory impairment that were the key features of AD neuropathology.

Mounts of evidence from postmortem indicated that the oxidative damage derived from intracellular oxidative stress is another early event of AD and high concentrations of Aβ oligomers can cause an increase in the production of reactive oxygen species (ROS) [9, 10]. Nevertheless, more evidence demonstrated that the interaction of Aβ especially with Cu^{2+} deliberately propels the generation of ROS, which would initiate synaptic damage and neurogenesis deficit eventually cause progressive neuropathology of the disease [9, 11].

Recently, a stilbene derivative florbetapir (**1**) and a thioflavin analogue flutemetamol (**2**) were approved to be Aβ imaging agents for the diagnosis of AD in patients

Correspondence: Prof. Ming-Kuan Hu, School of Pharmacy, National Defense Medical Center, Taipei 11490, Taiwan.
E-mail: hmk@ndmctsgh.edu.tw
Fax: +886 2 8792-3169

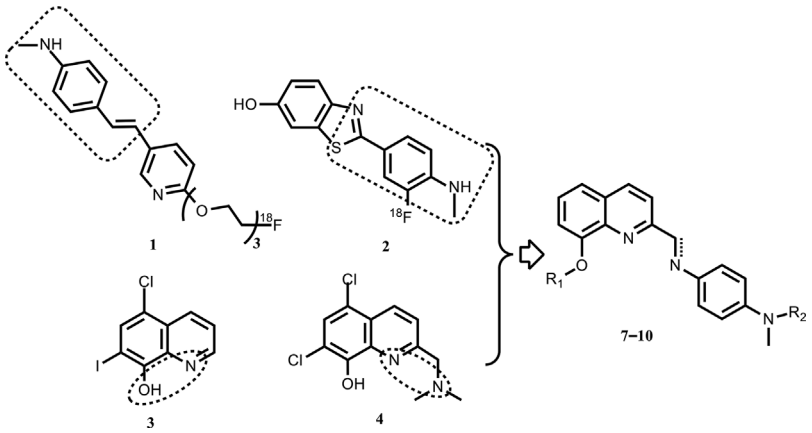

Figure 1. Design and chemical structures of multi-target modulators.

(Fig. 1) [12, 13], while certain hydroxyquinoline-based metal-protein attenuating compounds, for instance, clioquinol (**3**, CQ) and its derivative PBT2 (**4**) were conducted in clinic trials for the treatment of the disease [14, 15]. Structurally, the *N*-methylanilide or *N*,*N*-dimethylanilide moiety of these imaging agents has been indicated to play important role in Aβ recognition and interaction, by which these agents readily access and exert binding affinity to the Aβ aggregated fibrils. On the other hand, the hydroxyquinolinyl framework of the metal-protein attenuating compounds was assumed to furnish prevailing ability to chelate to the Aβ fibril-triggered metals and thus decreased the generation of the metal-mediated Aβ aggregation and prevented the subsequent neurotoxic damage. As described above, the perturbation of homeostasis of brain metal ions, especially copper and zinc, was detected to markedly entangle in the generation of the pathogenic Aβ assemblies and conspicuously drive the progressively pathological formation of the neurofibrillary tangles [11, 16]. Thus, metal dysregulation and the resulting oxidative stress are considered critical mechanisms of pathogenesis of AD [17, 18].

Regarding the evidence of these groundwork, much attention to the modulation of overloaded metal ions in the brain has recently been paid and pursued to be an intriguing approach for AD therapies [19, 20]. Our maneuver to explore the therapeutic strategies for AD is

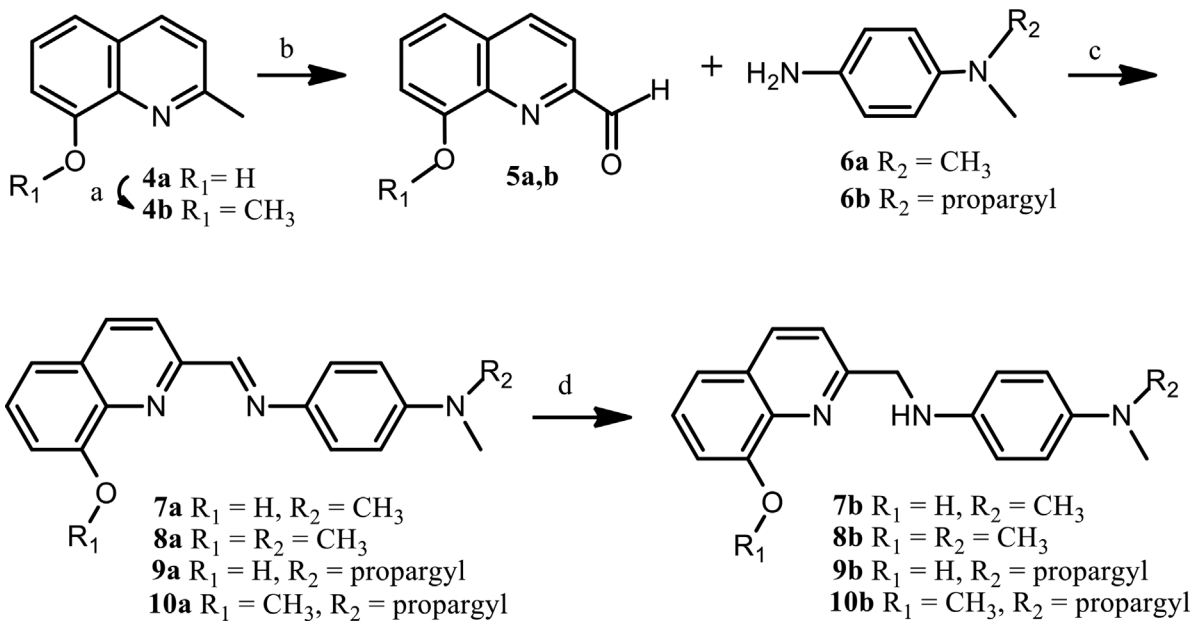

Scheme 1. Synthesis of hydroxyquinoline-based derivatives **7**–**10**. Reagents and conditions: (a) $(CH_3)_2SO_4$, K_2CO_3, r.t.; (b) SeO_2, 1,4-dioxane, reflux, 6 h; (c) HOAc, EtOH, r.t., 12 h; (d) $NaBH_4$, MeOH, r.t.

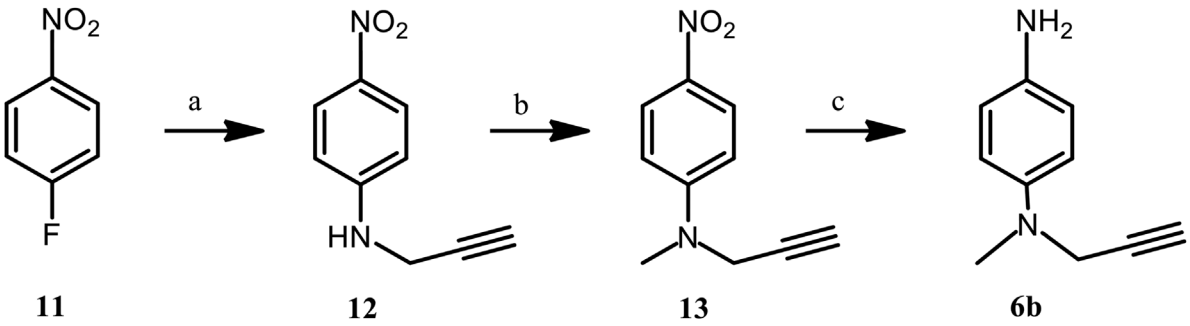

Scheme 2. Preparation of N^4-methyl-N^4-propargyl-phenylene-1,4-diamine. Reagents and conditions: (a) Propargylamine, K_2CO_3, DMSO, 12 h; (b) HCHO, HCOOH, reflux, 3 h; (c) $SnCl_2$, EtOH, reflux, 20 h.

to conjugate the *N*-methylanilide analogous moiety of the Aβ imaging agents to the core hydroxyquinoline of PBT2 and thus providing a type of new hydroxyquinoline-based derivatives as shown in Fig. 1. These multi-target modulators were expected to improve the effects on the metal-related Aβ aggregation through exhibiting metal chelating ability, modulation of Aβ assemblies, and antioxidant capacity.

Results and discussion

Chemistry

Synthesis of the designed hydroxyquinoline-based imines and their corresponding amines as new modulators was readily accomplished by starting with condensation of equimolar aldehydes and aromatic amines in acidic conditions to afford the aromatic imines, while subsequent reduction of these imines with sodium borohydride in mild conditions afforded the corresponding amines. Following the route depicted in Scheme 1, the commercially available 8-hydroxy-2-methylquinoline (**4a**) was readily methylated by reacting with dimethyl sulfate under basic condition to give 2-methyl-8-methoxy-quinoline (**4b**). The methylquinolines **4a**,**b** were each heated with selenium oxide in dioxane and water mixture under reflux to yield 2-quinolinecarbaldehydes **5a**,**b**, respectively [21]. Condensation of **5a**,**b** with dialkylanilides **6a**,**b** catalyzed by acetic acid afforded dimethylanilides **7a**, **8a** and propargylmethylanilides **9a**, **10a** in 48–72% yields. The subsequent reduction of these imines using sodium borohydride furnished a series of the corresponding amines **7b–10b** in good yields. In the meantime, the intermediate *N*-methylpropargylphenediamine (**6b**), required for the synthesis of compounds **9** and **10**, was prepared starting from 1-fluoro-4-nitrobenzene (**11**) as described in Scheme 2. Compound **11** was first condensed with propargylamine to give 4-nitro-*N*-propargylaniline (**12**) in 72% yield. Followed by using Eschweiler–Clarke reaction method [22], *N*-propargylaniline **12** was easily methylated in excess formic acid and formaldehyde to afford *N*-methyl-*N*-propargyl-4-nitroaniline (**13**) in 51% yield. Subsequent reduction of the nitroaniline **13** was carried out by using Bellamy's procedure [23] (stannous chloride in hot alcoholic solution) to give **6b** in 86% yield.

Table 1. Physical properties of compounds 7–10 compared to PBT2.

Descriptor[a)]	MW	clog*P*	HBA	HBD	PSA	logBB
PBT2	270.03	3.17	3	1	35.83	0.082
7a	291.13	3.48	4	1	48.72	−0.053
7b	293.15	3.19	4	2	47.86	−0.093
8a	305.15	3.36	3	0	37.19	0.090
8b	307.17	3.44	3	1	36.86	0.107
9a	315.14	3.86	4	1	48.19	0.004
9b	317.15	3.79	4	2	47.86	−0.002
10a	329.15	3.96	3	0	37.19	0.182
10b	331.17	4.04	3	1	36.86	0.199
Rules	≤ 500	≤ 5.0	≤ 10	≤ 5	≤ 90	> -0.1

[a)] MW: molecular weight; clog*P*: calculated logarithm of the octanol/water partition coefficient; HBD: hydrogen-bond donors; HBA: hydrogen-bond acceptors; PSA: polar surface area; $\text{logBB} = -0.0148 \times \text{PSA} + 0.152 \times \text{clog}P + 0.139$.

Biological evaluation

The development of the candidates for the CNS diseases therapies could be presciently assessed by the prediction of blood–brain barrier (BBB) penetration and drug-like criteria that were defined using Lipinski's rules [24] as described in Table 1, from which the capability to pass by BBB was checked by logBB values [25] and the Lipinski's rules pointed to molecular weight (MW), the octanol–water partition coefficient (logP), the number of hydrogen bond acceptor (HBA), and the number of hydrogen bond donor (HBD). In accordance with Lipinski's rules, the results of these descriptors provide evidence that these hydroxyquinoline-based derivatives possess the appropriate features to satisfy the drug-like criteria and retain the abilities for brain penetration with acceptable logBB values.

The modulating actions of these hydroxyquinoline-based derivatives on self-mediated Aβ aggregation were evaluated using the thioflavin T (ThT) fluorescence assay and the degree of Aβ aggregation was investigated principally by transmission electron microscopy (TEM), as generally reported previously. The well-studied PBT2 was used as a positive control. The relative ThT fluorescence unit (% of Aβ alone) shown in Fig. 2 indicated that these new compounds exhibited substantial inhibition of self-mediated Aβ aggregation (35–72% inhibition, Fig. 2A) as well as disaggregation of Aβ assembled fibrils (38–84% inhibition, Fig. 2B). Among them, compound **7a** is the most potent modulator of Aβ aggregation with much lower ThT units (28 and 16%, respectively), while PBT2 presented weak inhibition and disassembly on self-mediated Aβ aggregation as shown with higher ThT values (91 and 82%, respectively). The results suggested that featuring *N*,*N*-dialkylanilide moiety, these compounds possess the capability to recognize and interact with Aβ species, thus competing for ThT-binding sites on Aβ assembled fibrils, by which they not only prevent Aβ from aggregation but also disaggregate various Aβ fibrils. On the contrary, the marginal inhibition of PBT2 on self-mediated Aβ aggregation is possibly attributed to the short of the whole coordinative *N*,*N*-dialkylanilide group and thus barely interfered with ThT binding directly as observed previously [19]. The particular characterization of these hydroxyquinoline-based derivatives to inhibit Aβ aggregation and disaggregation of Aβ assemblies were further investigated by TEM images as shown in Fig. 3. In the inhibition (Fig. 3A), the condensed fibrils produced from incubation of Aβ alone changed to the loose fibers when incubated with PBT2, **7a**, or **7b**, while diverse clusters of short fibrils were present in the presence of compounds **8**–**10**. In the disaggregation (Fig. 3B), the images of Aβ species altered to loose fibrils in the presence of **7a**, while various clusters of short fibrils were observed for other compounds. On the groundwork of the ThT and TEM performance results, these new derivatives significantly influence Aβ aggregation.

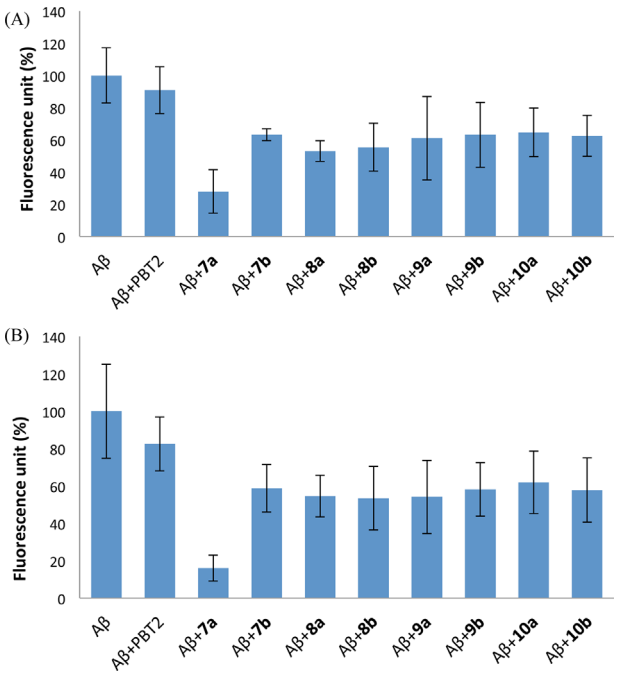

Figure 2. Plots of fluorescence intensity for the ThT assay on Aβ species: (A) Inhibition of self-mediated Aβ aggregation; (B) disaggregation of self-mediated Aβ assemblies.

To investigate the abilities of the hdroxyquinolinyl derivatives to modulate metal-induced Aβ aggregation, the corresponding ThT fluorescence assay was also conducted. In brief, the Aβ peptide was treated with 1 eq of $CuCl_2$ or $ZnCl_2$ for 2 min and then incubated with the tested compound for 1 day at 37°C. The relative ThT fluorescence unit (% of Aβ alone) was measured and the results are depicted in Fig. 4. The fluorescence of Aβ treated with Cu^{2+} and Zn^{2+} is increasing 52 and 13% more than that of Aβ alone, respectively, indicating that Cu^{2+} could substantially accelerate Aβ aggregations, while Zn^{2+} slightly brought up aggregations. When co-administrated with the test compound, the fluorescence of Aβ treated with Cu^{2+} groups tremendously decreased about 98% with *N*,*N*-dimethylanilide-containing derivatives **7a**,**b**, and **8a**,**b** and about 70% inhibition with *N*,*N*-methylpropargylanilide analogues **9a**,**b**, and **10a**,**b**, individually (Fig. 4A). In the case with Zn^{2+}, the fluorescence lowered about 70% for **7a**,**b**, and **8a**,**b** and around 20% for **9a**,**b**, and **10a**,**b**, while PBT2 committed relatively moderate inhibition of Aβ aggregation in both experiments (Fig. 4B). These results suggested that **7a**,**b**, and **8a**,**b** significantly recognize and influence the various Aβ species and thus effectively not only inhibit Cu^{2+}-mediated Aβ aggregation by capturing Cu^{2+} but also influence on the development of self-aggregation in the metal-free conditions. The results also reemphasized that the *N*,*N*-dimethylanilide moiety at the 2-position of the hydroxyquinoline-based framework would play an important role in Aβ recognition and interaction, while lack of the intact *N*,*N*-dimethylanilide group, PBT2 is blunt for Aβ recognition

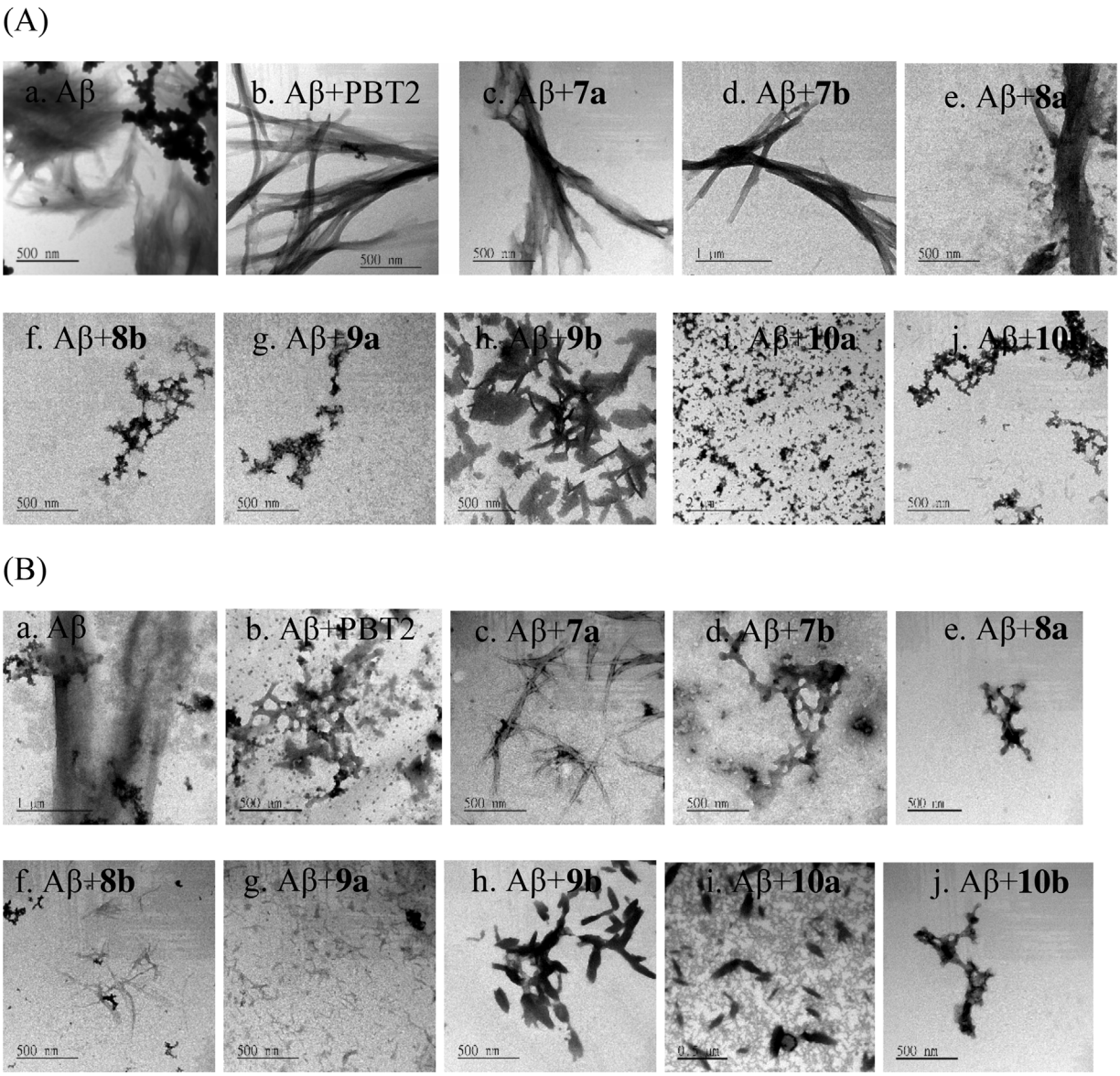

Figure 3. TEM image observations of hydroxyquinolinyl derivatives **7–10** for (A) inhibition of self-mediated Aβ aggregation, (B) disaggregation of self-mediated Aβ assemblies ([$A\beta_{42}$] = 25 μM, test compound = 50 μM, 37°C, 24 h). (a) Aβ, alone; (b) Aβ + PBT2; (c) Aβ + **7a**; (d) Aβ + **7b**; (e) Aβ + **8a**; (f) Aβ + **8b**; (g) Aβ + **9a**; (h) Aβ + **9b**; (i) Aβ + **10a**; (j) Aβ + **10b**.

and accessibility, thus showing decreased effects on inhibition of Aβ assembly. The morphology of Aβ species by TEM imaging was changed from condensed fibrils to looseness and relatively short fibrils for compounds **7a**,**b** and **8a**,**b** (Fig. 5A: d–g) and TEM images for the inhibition of Cu^{2+}-mediated (Fig. 5A) and Zn^{2+}-mediated (Fig. 5B) Aβ aggregations were probed and consistently verified the results of the ThT fluorescence assay.

The abilities of these derivatives to disaggregate metal-induced Aβ assembled fibrils were further investigated by the ThT assay. In the study, Aβ assembled fibrils were produced by reacting fresh Aβ with Cu^{2+} (1 eq) at 37°C for 24 h with constant agitation and the resulting sample was then treated with the test compound and incubated for additional 24 h at 37°C. The fluorescence of ThT assay was recorded in Fig. 6A. The results indicated that the *N*,*N*-dimethylanilide analogues **7a**,**b** and **8a**,**b** effectively disaggregated Aβ assembled fibrils compared to PBT2 (184 vs. 144% inhibition). The strong degradation of Aβ aggregated assembles revealed that these compounds not only disaggregated Cu^{2+}-induced Aβ fibrils

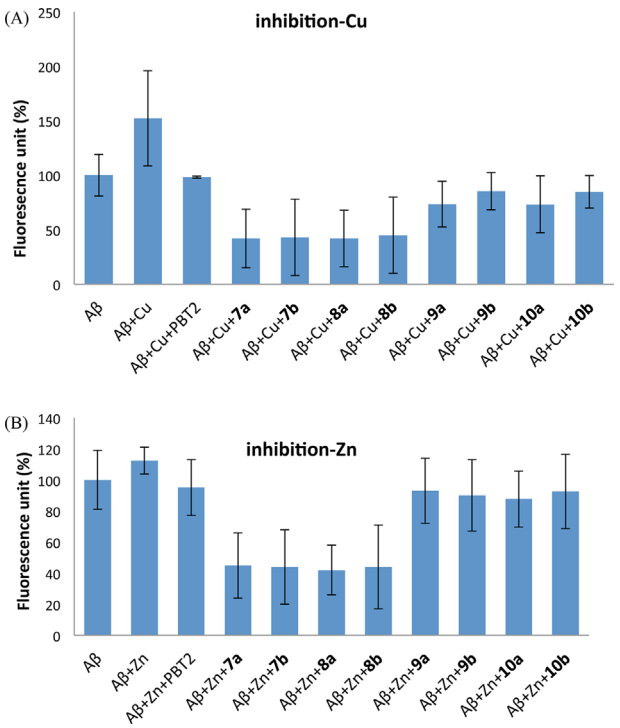

Figure 4. Plots of fluorescence intensity for the ThT assay on Aβ species: (A) Inhibition of Cu-mediated Aβ aggregation; (B) inhibition of Zn-mediated Aβ aggregation. Aβ (25 μM) was treated with 1 eq of Cu^{2+} or Zn^{2+} for 2 min followed by incubation with individual test compound (50 μM) for 24 h at 37°C.

but also disassembled the self-induced parts. Alternatively, similar profiles in the Zn^{2+}-induced experiment were investigated and indicated that **7a**,**b** and **8a**,**b** were slightly more potent than PBT2 on disaggregation of Zn^{2+}-triggered Aβ assembled fibrils with 2–15% lower fluorescence (Fig. 6B). The corresponding TEM images were provided in the Fig. 7 and found that the morphologies of Cu^{2+}-induced Aβ fibrils were altered to loosely short fibers (Fig. 7A: c–g) when treated with the substantial modulators PBT2, **7a**,**b** or **8a**,**b**, while the images were generally present as small and short clusters (Fig. 7A: h, i, j, and k) in Cu-triggered model or relatively condensed fibers (Fig. 7B: h–k) in Zn-induced patterns, when treated with compounds **9a**,**b** and **10a**,**b**.

The capabilities of the effective Aβ modulating hydroxyquinoline-based derivatives **7a**,**b** and **8a**,**b** to chelate Cu^{2+} and Zn^{2+} in comparison were examined by UV–Vis spectroscopies, from which the accumulative spectra were obtained from sequential addition of Cu^{2+} and Zn^{2+} to the methanolic solution of the test compound and in *vice versa*. As illustrated in Fig. 8A, the absorbance peaks of imine **7a** significantly shifted from around 275 and 415 nm to 305 and 490 nm and the absorbance dropped after the addition of Cu^{2+}, indicating the coordinated formation of **7a**-Cu^{2+}. The subsequent addition of Zn^{2+} to the solution clearly showed no change of the whole spectral and absorption patterns. While the same experiment with sequentially inverse addition of these metal ions was examined in Fig. 8B, a maximum absorption at 405 nm shifted to 500 nm and then significantly to 480 nm was observed. The results indicated that a small part of Zn^{2+} from **7a**-Zn^{2+} coordinated complex was replaced by Cu^{2+}, suggesting that the coordinating affinity of **7a** to Cu^{2+} is relatively stronger than that to Zn^{2+}. Similarly, the capabilities of compounds **7b** and **8a** coordinating to Cu^{2+} over to Zn^{2+} were observed, from which Cu^{2+} shifted the absorption peaks of the coordinated form of **7b**-Zn^{2+} and **8a**-Zn^{2+} from 480 to 520 nm and from 505 to 525 nm as depicted in the Figs. 9B and 10B, respectively, while **8b** showed no preferred chelation between both metals (Fig. 11B). The results revealed that the tridentate *N-N-O* moiety consisting of imino and 8-hydroxyquinolinyl moieties was the best pair for preferably chelating to Cu^{2+} and exhibited potent modulating effects on Aβ aggregation as above investigation, whereas tridentate composed of amino and 8-methoxyquinoinyl groups (i.e., **8b**) showed no preferable chelation to the metals and displayed less effective modulation on Aβ aggregation. The results also indicated that compounds **9a**,**b** and **10a**,**b**, which contain *N*,*N*-methylpropargylanilide but not *N*,*N*-dimethylanilide, showed much less reactive modulation toward self- or metal-mediated Aβ aggregation. Nevertheless, methylation of 8-hydroxyl group of **7a** did not abrogate the interaction and affinity toward metal-Aβ species as **8a** still showed substantial metal-chelation and reactivity on metal-mediated Aβ aggregations. Thus, the structural features of the hydroxyquinolinyl derivatives **7** and **8** underscore the importance of the *N*,*N*-dimethylanilide functionality for Aβ recognition and interaction and further influence metal-mediated Aβ aggregation processes.

Regarding the relative abilities for the effective Aβ modulators to possess antioxidant activity, a horseradish peroxidase (HRP)/Amplex Red assay [26] was carried out to evaluate their effects on the production of H_2O_2 by Cu^{2+}-bound Aβ in cell-free solutions [27]. As depicted in Fig. 12, imines **7a** and **8a** decreased 33–49% of Aβ- and Cu^{2+}-mediated formation of [H_2O_2] compared with the control set and were around sixfold more potent than PBT2 for preventing Cu^{2+}-mediated Aβ from generating the ROS. Nevertheless, the amino analogue **7b** still showed more potent anti-oxidant activity than PBT2. The results indicated that the tridentate imines **7a** and **8a** can effectively reduce the production of H_2O_2 by Cu^{2+}-bound Aβ, suggesting that structured with *N*,*N*-dimethylanilide as Aβ recognition moiety and tridentate skeleton for metal chelation, the new hydroxyquinolines possess Aβ interaction capability and alleviation of metal-mediated Aβ toxicity. While PBT2 showed almost no inhibitory effects on Aβ/Cu^{2+}-mediated H_2O_2 production, its lower chelating ability to metal as above investigations on spectroscopic experiments would reflect its weak effects on prevention of H_2O_2 production. Previously,

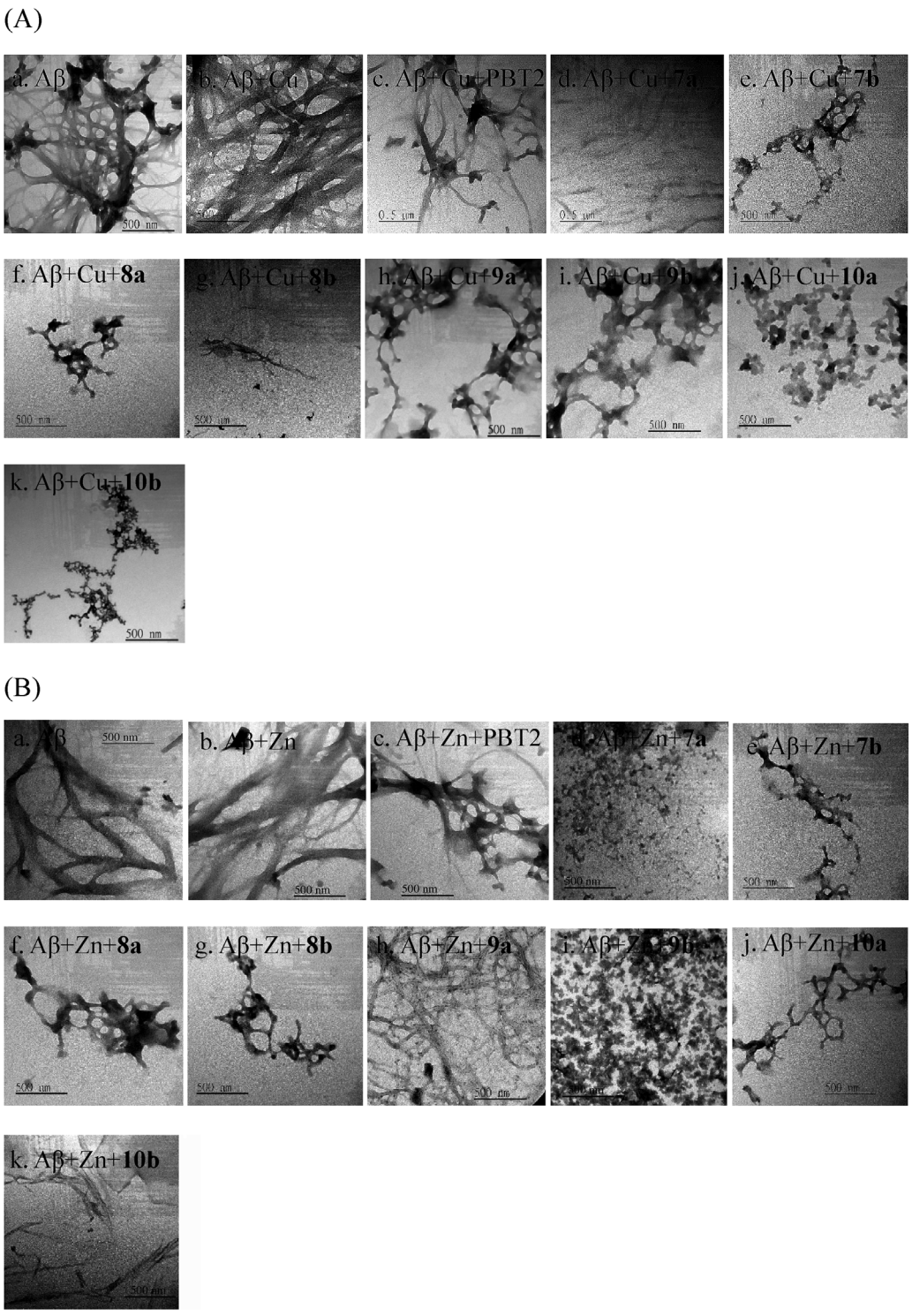

Figure 5. TEM image observations of hydroxyquinolinyl derivatives **7–10** for (A) inhibition of Cu-mediated Aβ aggregation: (a) Aβ, alone; (b) Aβ + Cu; (c) Aβ + Cu + PBT2; (d) Aβ + Cu + **7a**; (e) Aβ + Cu + **7b**; (f) Aβ + Cu + **8a**; (g) Aβ + Cu + **8b**; (h) Aβ + Cu + **9a**; (i) Aβ + Cu + **9b**; (j) Aβ + Cu + **10a**; (k) Aβ + Cu + **10b**; (B) inhibition of Zn-mediated Aβ aggregation: (a) Aβ, alone; (b) Aβ + Zn; (c) Aβ + Zn + PBT2; (d) Aβ + Zn + **7a**; (e) Aβ + Zn + **7b**; (f) Aβ + Zn + **8a**; (g) Aβ + Zn + **8b**; (h) Aβ + Zn + **9a**; (i) Aβ + Zn + **9b**; (j) Aβ + Zn + **10a**; (k) Aβ + Zn + **10b**. ([$A\beta_{42}$] = 25 μM, test compound = 50 μM, [Cu^{2+}] = [Zn^{2+}] = 25 μM, 37°C, 24 h).

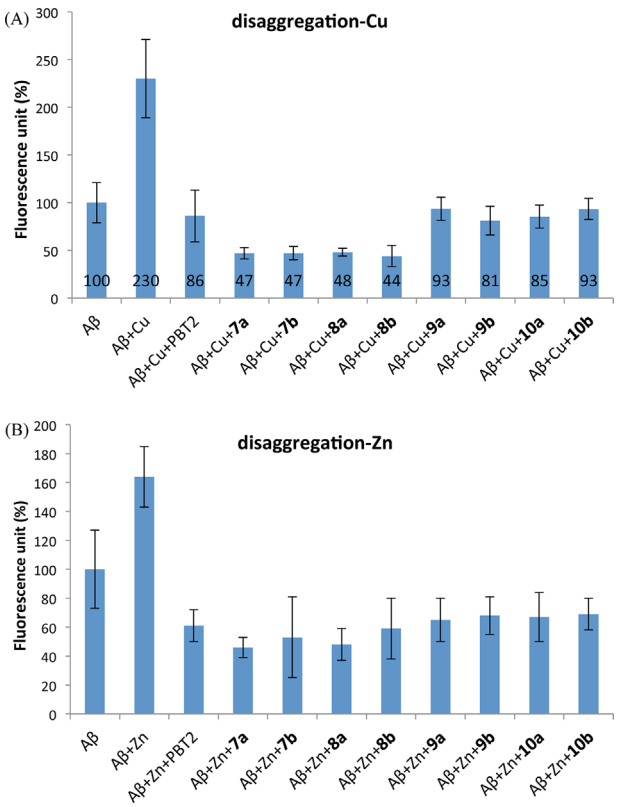

Figure 6. Plots of the fluorescence intensity of ThT in the presence of Aβ species: (A) Disaggregation of Cu-triggered Aβ assembled fibrils; (B) disaggregation of Zn-triggered Aβ assembled fibrils. Aβ (25 μM) was incubated with 1 eq of Cu^{2+} or Zn^{2+} for 24 h followed by treating with the test compound (50 μM) and incubation for additional 24 h at 37°C.

Lim and co-workers reported a potent imine modulator of Aβ aggregation but likely showed poor biocompatibility due to its limited aqueous stability for the imine moiety. An amine derivative was further described to address the problem [28]. Here, in addition to **7a**, the amine analogue **7b** showed promising reactivity toward metal-mediated Aβ aggregations and moderate free radical scavenging effects and would improve aqueous stability and solubility. Taken together, these results suggest that the imine **7a** and its amino analogue **7b** furnished multifunctional abilities for modulation of various Aβ models and can be valuable for further study.

In this study, we demonstrated that on the basis of the key structural features of the established metal-protein attenuating compounds and the imaging agent, the multifunctional modulators **7a** and its amino analogue **7b** were obtained by rational conjugation of the core hydroxyquinoline and the *N*,*N*-dimethylanilide scaffold. The *N*,*N*,O-tridentate derivatives **7a** and **7b** not only exhibited effective inhibition of Aβ aggregation in the absence and presence of metal ions but also showed significant abilities to disassemble metal-induced Aβ aggregates at pH 7.4. Moreover, both **7a** and **7b** also exerted noticeable antioxidant properties with lowering H_2O_2 production triggered by Cu^{+2}-mediated Aβ. These results demonstrated that the new hydroxyqinolinyl imine **7a** and amine **7b** possess potentials for AD therapeutic and are considerable to be promising lead molecules toward the candidates for the devastating disease.

Experimental

Chemistry

Melting points were recorded by Fargo MP-1D apparatus in open capillary tubes and are uncorrected. The NMR spectra were recorded on Varian Gemini-300FT or Agilent 400-MR spectrometers for ^1H and ^{13}C spectra and reported in parts per million with respect to tetramethylsilane as an internal standard. ^1H NMR coupling constants (*J* values) were listed in Hertz (Hz) and spin multiplicities are reported as singlet (s), doublet (d), triplet (t), quartet (q), multiplet (m), and broad (br). Elemental analyses were performed using a PerkinElmer 240 EA analyzer. Fast atom bombardment mass spectra (FABMS) were obtained from a Finnigan MAT-95XL mass spectrometer. Chromatography refers to flash chromatography on silica gel (silica gel 60, 230–400 mesh ASTM, E. Merck, Darmstadt, Germany). UV spectra were observed using a Shimadzu UV-2450 UV–Vis recording spectrophotometer. Transmission electron microscopes (TEM) were probed using a Jeol Electron Microscope JEM-1230. Fluorescence was obtained from a fluorophotometer Infinite M200. PBT2 (5,7-dichloro-2-[(dimethylamino)methyl]quinolin-8-ol) was prepared starting from commercial 5,7-dichloro-8-hydroxy-quinaldine in accordance with the procedure reported previously [29].

Please see the Supporting Information for the InChI codes of the new compounds.

*8-Methoxy-2-methylquinoline (**4b**)*

To a mixture of **4a** (1.59 g, 10 mmol), potassium carbonate (1.658 g, 12 mmol), dimethyl sulfate (0.95 mL, 10 mmol) in 40 mL of DMF was stirred at room temperature for 18 h. The reaction mixture was diluted with added water (50 mL) and extracted with ethyl acetate (60 mL). The organic layer was separated, dried over $MgSO_4$, and concentrated. The residue was purified by silica gel column chromatography to give **4b** (1.26 g, 73%) as a white powder. TLC $R_f = 0.44$ (EtOAc/*n*-hexane = 1:1); mp 127−130°C (lit. [30] 126–127°C); ^1H NMR (400 MHz, $CDCl_3$) δ 2.80 (s, 3H, C<u>H</u>$_3$), 4.08 (s, 3H, C<u>H</u>$_3$), 7.03 (d, $J = 7.6$ Hz, 1H, aromatic <u>H</u>), 7.31–7.42 (m, aromatic <u>H</u>), 8.02 (d, $J = 8.4$ Hz, aromatic <u>H</u>).

*8-Hydroxyquinoline-2-carbaldehyde (**5a**)*

To a mixture of SeO_2 (1.9 g, 17 mmol) in 1,4-dioxane (30 mL) was added 8-hydroxy-2-methylquinoline (**4a**, 1.6 g, 10 mmol) at room temperature and heated under reflux at 85°C for 8 h. The reaction mixture was filtered and washed with

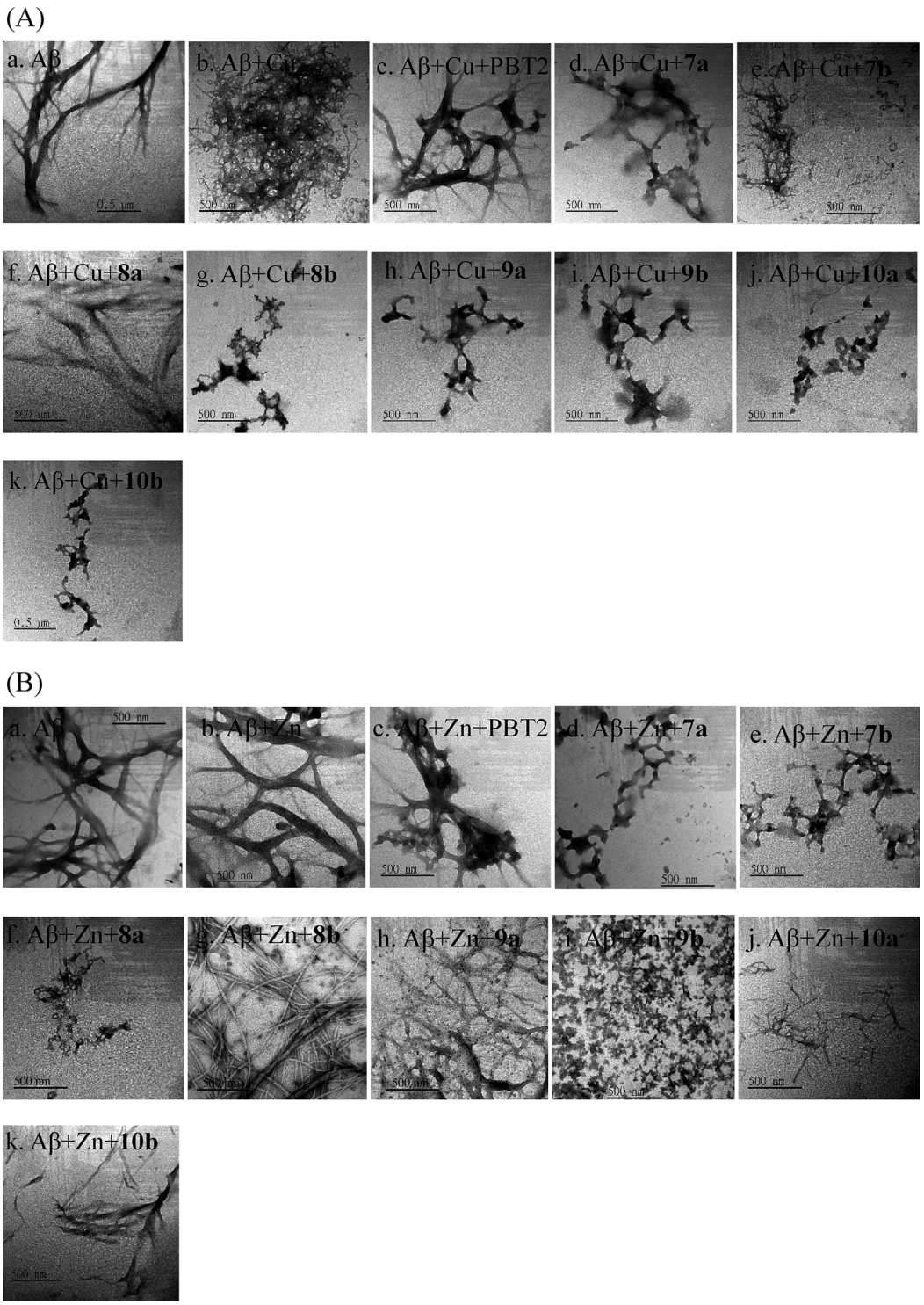

Figure 7. TEM image observations of hydroxyquinolinyl derivatives **7–10** for (A) disaggregation of Cu-induced Aβ assembled fibrils: (a) Aβ, alone; (b) Aβ + Cu; (c) Aβ+ Cu + PBT2; (d) Aβ + Cu + **7a**; (e) Aβ + Cu + **7b**; (f) Aβ + Cu + **8a**; (g) Aβ + Cu + **8b**; (h) Aβ + Cu + **9a**; (i) Aβ + Cu + **9b**; (j) Aβ + Cu + **10a**; (k) Aβ + Cu + **10b**; (B) disaggregation of Zn-induced Aβ assembled fibrils: (a) Aβ, alone; (b) Aβ + Zn; (c) Aβ + Zn + PBT2; (d) Aβ + Zn + **7a**; (e) Aβ + Zn + **7b**; (f) Aβ + Zn + **8a**; (g) Aβ + Zn + **8b**; (h) Aβ + Zn + **9a**; (i) Aβ + Zn + **9b**; (j) Aβ + Zn + **10a**; (k) Aβ + Zn + **10b**. ([$A\beta_{42}$] = 25 μM, tested compound = 50 μM, [Cu^{2+}] = [Zn^{2+}] = 25 μM, 37°C, 24 h).

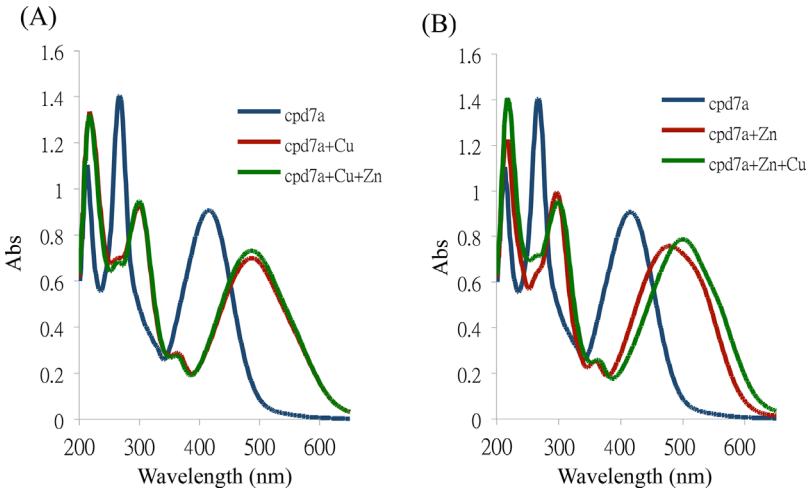

Figure 8. UV spectra of (A) **7a** (50 μM) alone (blue line), treated with $CuCl_2$ (50 μM) (red line), and followed by $ZnCl_2$ (50 μM) (green line); (B) **7a** (50 μM) alone, treated with $ZnCl_2$ (50 μM), and followed by $CuCl_2$ (50 μM), in MeOH.

dichloromethane (3 × 30 mL). The combined filtrates were evaporated under pressure and the residue was purified by silica gel column chromatography to give **5a** (0.89 g, 51%) as straw yellow solid. TLC $R_f = 0.56$ (EtOAc/*n*-hexane = 1:3); mp 101–103°C (lit. [31] 98–99.7°C); ^{1}H NMR (400 MHz, $CDCl_3$) δ 7.27 (dd, $J = 1.2$, 7.6 Hz, 1H, aromatic H), 7.41 (dd, $J = 1.2$, 8.2 Hz, 1H, aromatic H), 7.61 (t, $J = 7.6$, 8.4 Hz, 1H, aromatic H), 8.03 (d, $J = 8.4$ Hz, 1H, aromatic H), 8.16 (s, 1H, OH), 8.29 (d, $J = 8.4$ Hz, 1H, aromatic H), 10.19 (s, CHO).

*8-Methoxyquinoline-2-carbaldehyde (**5b**)*

To a mixture of SeO_2 (0.59 g, 5.4 mmol) in 1,4-dioxane (35 mL) was added **4b** (0.33 g, 3 mmol) at room temperature and heated with reflux at 85°C for 6 h. The reaction mixture was filtered and washed with dichloromethane (2 × 20 mL). The combined organic layers were evaporated under pressure and the residue was purified by silica gel column chromatography to give **5b** (0.29 g, 78%) as a yellow powder. TLC $R_f = 0.35$ (EtOAc/*n*-hexane = 1:3); mp 102–104°C (lit. [32] 103–104°C); ^{1}H NMR (300 MHz, $CDCl_3$) δ 4.16 (s, 3H, CH_3), 7.16 (d, $J = 8.4$ Hz, 1H, aromatic H), 7.47 (d, $J = 8$ Hz, 3H, aromatic H), 7.60–7.64 (t, $J = 8$ Hz, aromatic H), 8.06 (d, $J = 8.4$ Hz, aromatic H), 8.28 (d, $J = 0.6$ Hz, aromatic H), 10.31 (s, CHO).

*(E)-2-(4-(Dimethylamino)phenylimino)methyl)quinolin-8-ol (**7a**)*

A mixture of carbaldehyde **5a** (1.24 g, 7.16 mmol), phenylenediamine (**6a**, 0.97 g, 7.16 mmol), and trace of acetic acid in methanol (20 mL) was stirred at room temperature for 3 h. The reaction mixture was filtered. The resulting residue was collected and washed with methanol to give **2** (1.27 g, 61%) as dark yellow solid; TLC $R_f = 0.37$ (EtOAc/*n*-hexane = 1:2); mp 165−166°C; UV λmax (MeOH) nm (log ε): 212 (1.094), 267 (1.405), 415 (0.907); IR (cm^{-1}): 3035, 2885; ^{1}H NMR (300 MHz, $CDCl_3$) δ 3.02 (6H, s, $-CH_3$), 6.78 (2H, d, $J = 9.0$ Hz, Ar–H), 7.19 (1H, dd, $J = 7.65$, 1.2 Hz, Ar–H), 7.35 (1H, d, $J = 8.4$ Hz, Ar–H), 7.43 (2H, d, $J = 8.4$ Hz, Ar–H), 7.42–7.50 (1H, m, Ar–H), 8.19 (1H, d, $J = 8.7$ Hz, Ar–H), 8.48 (1H, d, $J = 8.4$ Hz, Ar–H), 8.79 (1H, s, –CH=N); ^{13}C-NMR (75 MHz, $CDCl_3$) δ 40.4, 110.3, 112.4, 117.8, 119.1, 123.0, 128.4, 128.7, 136.2, 137.8, 139.0, 150.2, 152.3, 153.3, 154.5; FABMS: m/z 292.0 $[M+H]^+$; HRFABMS: calcd. for $C_{18}H_{18}N_3$ $[M+H]^+$ 292.1450, found, 292.1448.

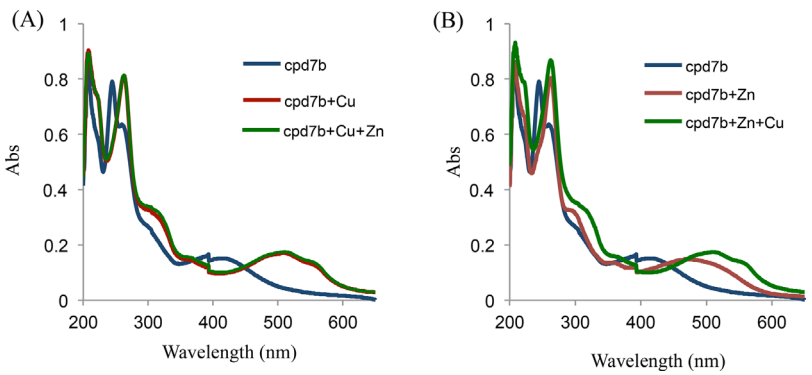

Figure 9. UV spectra of (A) **7b** (50 μM) alone (blue line), treated with $CuCl_2$ (50 μM) (red line), and followed by $ZnCl_2$ (50 μM) (green line); (B) **7b** (50 μM) alone, treated with $ZnCl_2$ (50 μM), and followed by $CuCl_2$ (50 μM), in MeOH.

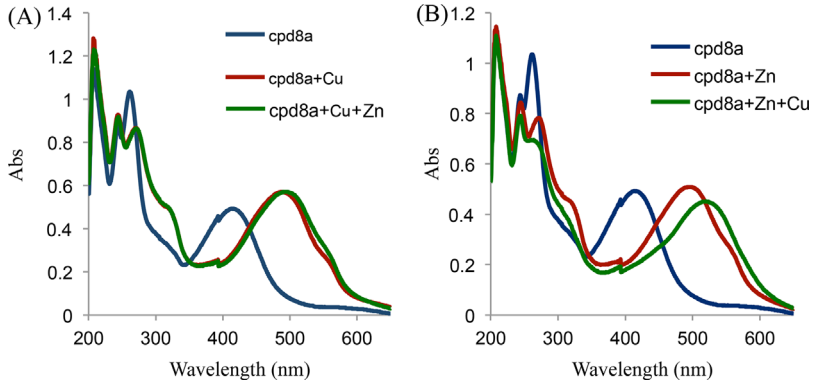

Figure 10. UV spectra of (A) **8a** (50 μM) alone (blue line), treated with $CuCl_2$ (50 μM) (red line), and followed by $ZnCl_2$ (50 μM) (green line); (B) **8a** (50 μM) alone, treated with $ZnCl_2$ (50 μM), and followed by $CuCl_2$ (50 μM), in MeOH.

*2-((4-(N,N-Dimethylamino)phenylamino)methyl)quinolin-8-ol (**7b**)*

A mixture of **7a** (0.76 g, 2.6 mmol) and sodium borohydride (1 g, 26.4 mmol) in MeOH (40 mL) was stirred for 1 h at room temperature. The reaction mixture was quenched by water (50 mL) and extracted with Et_2O (4 × 50 mL). The combined organic layers were separated and dried over $MgSO_4$ to give compound **7b** as brown oil (yield 78%). TLC R_f = 0.46 (EtOAc/*n*-hexane = 1:1); ^{1}H NMR (300 MHz, $CDCl_3$) δ 2.28 (s, 6H, C<u>H</u>$_3$), 4.60 (s, 2H, C<u>H</u>$_2$), 6.67–6.76 (m, 4H, aromatic <u>H</u>), 7.18 (dd, *J* = 1.2, 7.5 Hz, 1H, aromatic <u>H</u>), 7.28 (d, *J* = 8.1 Hz, 1H, aromatic <u>H</u>), 7.40–7.45 (t, *J* = 7.5, 8.1 Hz, 1H, aromatic <u>H</u>), 7.51 (d, *J* = 8.4 Hz, 1H, aromatic <u>H</u>), 8.1 (d, *J* = 8.4 Hz, 1H, aromatic <u>H</u>); ^{13}C-NMR (75 MHz, $CDCl_3$) δ 154.75, 153.61, 152.57, 150.49, 139.32, 137.98, 136.36, 128.91, 128.53, 123.16, 119.26, 117.90, 112.66, 110.36, 41.97, 40.44; IR (cm^{-1}): 3423.3, 1614.3, 1517.9; HRMS (EI): calcd. for $C_{18}H_{19}N_3O$ $[M]^+$, 293.1524; found, 293.1528.

*(E)-N^1-((8-Methoxyquinolin-2-yl)methylene)-N^4,N^4-dimethylbenzene-1,4-diamine (**8a**)*

A mixture of aldehyde **5b** (0.95 g, 5 mmol), *N,N*-dimethyl-*p*-phenylenediamine (**6a**, 0.75 g, 5.5 mmol), and three drops of acetic acid in ethanol (20 mL) was stirred at room temperature for 6 h and then concentrated in vacuum. The residue was purified by silica gel column chromatography to give compound **8a** (0.79 g, 52%) as orange oil. TLC R_f = 0.3 (EtOAc/*n*-hexane = 1:1); ^{1}H NMR (400 MHz, $CDCl_3$) δ 3.01 (s, 6H, C<u>H</u>$_3$), 4.13 (s, 3H, C<u>H</u>$_3$), 6.77 (d, *J* = 8.8 Hz, 2H, aromatic <u>H</u>), 7.09 (d, *J* = 7.2 Hz, 1H, aromatic <u>H</u>), 7.43–7.49 (m, 4H, aromatic <u>H</u>), 8.18 (d, *J* = 8.8 Hz, 1H, aromatic <u>H</u>), 8.42 (d, *J* = 8.4 Hz, 1H, aromatic <u>H</u>), 8.98 (s, 1H, C<u>H</u> = N); ^{13}C-NMR (100 MHz, DMSO) δ 155.66, 155.54, 150.29, 154.88, 139.96, 139.23, 136.38, 127.53, 123.38, 119.74, 119.19, 116.68, 115.68, 112.66, 108.05, 56.28, 40.64; IR (cm^{-1}): 3647.1, 1683.7, 1652.9, 1506.3; HRMS (EI): calcd. for $C_{19}H_{19}N_3O$ $[M]^+$, 305.1524; found, 305.1525.

*N^1-((8-Methoxyquinolin-2-yl)methyl)-N^4,N^4-dimethylbenzene-1,4-diamine (**8b**)*

A mixture of imine **8a** (0.76 g, 2.6 mmol) and sodium borohydride (1 g, 26.4 mmol) in methanol (40 mL) was stirred 2 h at room temperature. The reaction was quenched by water (50 mL) and then extracted with ethyl acetate (4 × 50 mL). The combined organic layers were dried over anhydrous $MgSO_4$ to give **8b** (0.51 g, 64%) as orange yellow oil. TLC R_f = 0.35 (EtOAc/*n*-hexane = 1.5:1); ^{1}H NMR (400 MHz, $CDCl_3$) δ 2.77 (s, 6H, C<u>H</u>$_3$), 4.11 (s, 3H, C<u>H</u>$_3$), 4.67 (s, C<u>H</u>$_2$), 6.65–6.74 (m, 4H, aromatic <u>H</u>), 7.07 (dd, *J* = 0.8 Hz, 7.6 Hz, 1H,

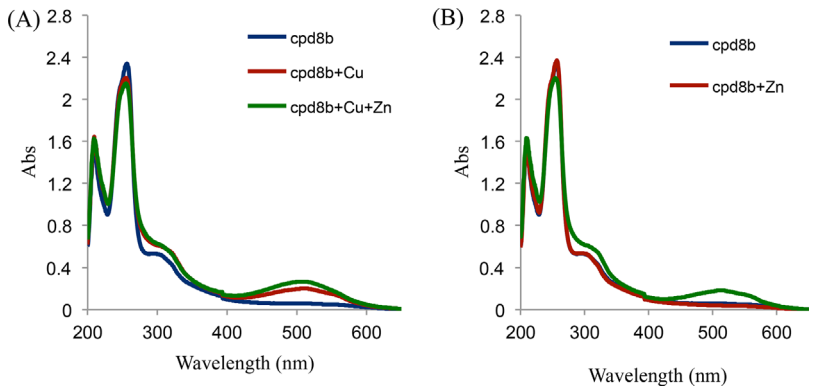

Figure 11. UV spectra of (A) **8b** (50 μM) alone (blue line), treated with $CuCl_2$ (50 μM) (red line), and followed by $ZnCl_2$ (50 μM) (green line); (B) **8b** (50 μM) alone, treated with $ZnCl_2$ (50 μM), and followed by $CuCl_2$ (50 μM), in MeOH.

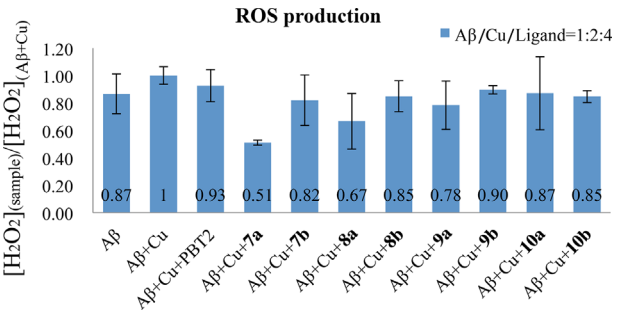

Figure 12. Effects of the hydroxyquinolinyl derivatives on the production of H_2O_2 from Aβ treated with Cu^{2+}, evaluated on a HRP/Amplex-Red assay. The concentrations of [Aβ] = 200 nM, [Cu^{2+}] = 400 nM, [chelator] = 800 nM, [ascorbate] = 10 μM, [Amplex Red] = 50 μM, and [HRP] = 0.1 U/mL, and the measurement set at $\lambda_{Ex/Em}$ = 530/590 nm.

aromatic H), 7.37 (dd, *J* = 1.2 Hz, 8.4 Hz, 1H, aromatic H), 7.44 (t, *J* = 8 Hz, 1H, aromatic H), 7.57 (d, *J* = 8.4 Hz, 1H, aromatic H), 8.07 (d, *J* = 8.8 Hz, 1H, aromatic H); ^{13}C-NMR (100 MHz, DMSO) δ 159.41, 154.94, 144.11, 140.41, 139.56, 136.64, 128.46, 126.15, 120.24, 119.56, 115.83, 114.44, 107.89, 56.07, 51.29, 42.21; IR (cm^{-1}): 3444.6, 1558.4, 1506.3; HRMS(EI): calcd. for $C_{19}H_{21}N_3O$ $[M]^+$ 307.1680; found, 307.1526.

*4-Nitro-N-(propargyl)aniline (**12**)*
A mixture of 4-fluoro-1-nitrobenzene (**11**, 0.42 g, 3 mmol), propargylamine (0.16 mL, 3 mmol), and potassium carbonate (0.5 g, 3.6 mmol), and triethylamine (0.5 mL) was dissolved in DMSO (10 mL) and stirred overnight at 50°C. The reaction mixture was then poured into ice water and the resulting precipitate was collected by filtration and washed with water. The residue was purified with 2-propanol to give **12** (0.37 g, 72%) as white solid. TLC R_f = 0.43 (EtOAc/*n*-hexane = 1:4); mp 128–132°C; ^{1}H NMR (400 MHz, $CDCl_3$) δ 4.03 (q, *J* = 2.4 Hz, 2H, CH_2CCH), 4.69 (br, 2H, NH), 6.64 (d, *J* = 9.8 Hz, 2H, aromatic H), 8.12 (d, *J* = 7.2 Hz, 2H, aromatic H). IR (cm^{-1}): 3404.1, 3247.9, 1600.8, 1521.7; MS (EI): 172 $[M]^+$.

*4-Nitro-N-methyl-N-(propargyl)aniline (**13**)*
A mixture of **12** (0.35 g, 2 mmol), formaldehyde (10 mmol), and formic acid (6 mmol) was heated under reflux for 3 h and concentrated *in vacuo*. The crude residue was purified by silica gel column chromatography to get **13** (0.19 g, 51%) as yellow solid. TLC R_f = 0.56 (EtOAc/hexane = 1:4); mp 93–95°C (lit. [33] 93–95°C); ^{1}H NMR (400 MHz, $CDCl_3$) δ 2.26 (t, *J* = 2.4 Hz, 1H, CCH) 3.14 (s, 3H, CH_3), 4.15 (d, *J* = 2.4 Hz, 2H, CH_2CCH), 6.75 (d, *J* = 7.4 Hz, 2H, aromatic H), 8.16 (d, *J* = 7.4 Hz, 2H, aromatic H); MS (EI): 186 $[M]^+$.

*N^1-Methyl-N^1-(prop-2-ynyl)benzene-1,4-diamine (**6b**)*
A mixture of **13** (0.2 g, 0.91 mmol) and tin(II) chloride dihydrate (1 g, 4.5 mmol) in 20 mL of ethanol was stirred and heated under reflux for 21 h. The reaction mixture was cooled and neutralized by aqueous sodium hydroxide solution in an ice bath. The resulting precipitate was removed and the aqueous filtrate was extracted with ethyl acetate (2 × 20 mL). The combined organic layers were washed with brine and dried over anhydrous $MgSO_4$. After concentration, the residue was purified by silica gel chromatography to give **6b** (0.13 g, 86%) as brown oil [32]. TLC R_f = 0.59 (EtOAc/*n*-hexane = 1:1); ^{1}H NMR (400 MHz, $CDCl_3$) δ 2.17 (t, *J* = 2.4 Hz, 1H, CCH), 2.86 (s, 3H, CH_3), 3.30–3.60 (bs, 2H, NH_2), 3.93 (d, *J* = 2.4 Hz, 2H, CH_2CCH), 6.67 (d, *J* = 6.6 Hz, 2H, aromatic H), 6.79 (d, *J* = 6.4 Hz, 2H, aromatic H).

*(E)-2-((4-(N-Methyl-N-propargyl)amino)phenylimino)-methyl)quinolin-8-ol (**9a**)*
To a mixture of aldehyde **5a** (0.54 g, 3.1 mmol), phenylenediamine **6b** (0.69 g, 4.3 mmol), and trace of acetic acid in methanol (20 mL) was stirred at room temperature for 8 h. The reaction mixture was filtered and the collected solid was washed with methanol to give **9a** (0.47 g, 48%) as yellow green solid. TLC R_f = 0.39 (EtOAc/*n*-hexane = 1:3); mp 135°C; ^{1}H NMR (400 MHz, $CDCl_3$) δ 2.22 (t, *J* = 2.4 Hz, 1H, CCH), 3.06 (s, 3H, CH_3), 4.11 (d, *J* = 2.4 Hz, 2H, CH_2CCH), 6.91 (d, *J* = 8.8 Hz, 2H, aromatic H), 7.20 (d, *J* = 7.6 Hz, 1H, aromatic H), 7.36 (d, *J* = 8.4 Hz, 1H, aromatic H), 7.44 (d, *J* = 9.2 Hz, 1H, aromatic H), 7.49 (t, *J* = 8 Hz, 1H, aromatic H), 8.21 (d, *J* = 8.8 Hz, 1H, aromatic H), 8.37 (d, *J* = 8.4 Hz, 1H, aromatic H), 8.80 (s, 1H, CH=N); ^{13}C-NMR (100 MHz, $CDCl_3$) δ 156.03, 153.40, 152.61, 148.86, 140.93, 138.02, 136.60, 129.08, 128.83, 123.14, 119.41, 115.07, 114.50, 110.58, 79.18, 72.39, 42.63, 38.90; IR (cm^{-1}): 3419.6, 3300.5, 1683.7, 1616.2, 1508.2; HRMS (EI): calcd. for $C_{20}H_{17}N_3O$ $[M]^+$, 315.1368; found, 315.1362.

*2-((4-(N-Methyl-N-propargyl)amino)phenylamino)methyl)-quinolin-8-ol (**9b**)*
A mixture of imine **9a** (0.47 g, 1.5 mmol) and sodium borohydride (0.4 g, 10.6 mmol) in methanol (30 mL) was stirred for 10 min at 0°C. After 1 h at room temperature, the reaction was quenched by water (40 mL) and extracted with ethyl acetate (4 × 40 mL). The organic layers were separated and dried over anhydrous $MgSO_4$ to give compound **9b** (yield, 72%) as yellow oil. TLC R_f = 0.25 (EtOAc/*n*-hexane = 1:2); ^{1}H NMR (400 MHz, $CDCl_3$) δ 2.17 (t, *J* = 2.4 Hz, 1H, CCH), 2.86 (s, 3H, CH_3), 3.94 (d, *J* = 2.4 Hz, 2H, CH_2CCH), 4.59 (s, CH_2), 6.69 (d, *J* = 8.8 Hz, 2H, aromatic H), 6.84 (d, *J* = 8.8 Hz, 2H, aromatic H), 7.19 (dd, *J* = 0.8 Hz, 7.6 Hz, 1H, aromatic H), 7.31 (d, *J* = 8.4 Hz, 1H, aromatic H), 7.42 (t, *J* = 8 Hz, 1H, aromatic H), 7.51 (d, *J* = 8.8 Hz, 1H, aromatic H), 8.1 (d, *J* = 8.8 Hz, 1H, aromatic H); ^{13}C-NMR (100 MHz, $CDCl_3$) δ 157.87, 151.82, 142.16, 141.43, 137.51, 136.89, 127.60, 127.31, 123.05, 120.67, 117.89, 117.73, 114.36, 110.31, 79.51, 72.41, 50.69, 44.22, 39.56; IR (cm^{-1}): 3419.6, 3300.0, 1618.2, 1508.2; HRMS (EI): calcd. for $C_{20}H_{19}N_3O$ $[M]^+$, 317.1524; found, 317.1527.

*(E)-N^1-((8-Methoxyquinolin-2-yl)methylene)-N^4-methyl-N^4-(propargyl)phenylene-1,4-diamine (**10a**)*
To a mixture of aldehyde **5b** (0.62 g, 3.3 mmol), phenylenediamine **6b** (0.64 g, 4 mmol), trace of acetic acid in methanol

(20 mL) was stirred at room temperature for 4 h. The reaction mixture was filtered and the resulting residue was purified by silica gel column chromatography to give compound **10a** (0.68 g, 63%) as brown oil. TLC $R_f = 0.44$ (EtOAc/*n*-hexane = 1:1); ^{1}H NMR (400 MHz, $CDCl_3$) δ 2.21 (t, $J = 2.4$ Hz, 1H, CC<u>H</u>), 3.04 (s, 3H, C<u>H</u>$_3$), 4.10 (d, $J = 2.4$ Hz, 2H, C<u>H</u>$_2$CCH), 4.1 (s, C<u>H</u>$_2$), 4.67 (s, 2H, C<u>H</u>$_2$), 6.89 (d, $J = 7$ Hz, 2H, aromatic <u>H</u>), 7.09 (d, $J = 7.6$ Hz, 1H, aromatic <u>H</u>), 7.41–7.51 (m, 4H, aromatic <u>H</u>), 8.18 (d, $J = 8.4$ Hz, 1H, aromatic <u>H</u>), 8.42 (d, $J = 8.4$ Hz, 1H, aromatic <u>H</u>), 8.97 (s, 1H, C<u>H</u>=N); ^{13}C-NMR (100 MHz, $CDCl_3$) δ 156.72, 155.51, 154.64, 148.59, 140.76, 139.90, 136.44, 129.91, 127.66, 123.21, 119.71, 119.19, 114.33, 108.05, 79.12, 72.27, 56.27, 42.47, 38.75; IR (cm^{-1}): 3384.8, 1635.5, 1541.0, 1508.2; HRMS (EI): calcd. for $C_{21}H_{19}N_3O$ $[M]^+$, 329.1524; found, 329.1522.

*N^1-((8-Methoxyquinolin-2-yl)methyl)-N^4-methyl-N^4-(propargyl)benzene-1,4-diamine (**10b**)*

A mixture of imine **10a** (0.49 g, 1.48 mmol) and sodium borohydride (0.38, 10.0 mmol) in methanol (30 mL) was stirred for 10 min at 0°C. After 2 h at room temperature, the reaction was quenched by water (40 mL) and extracted with ethyl acetate (4 × 40 mL) four times. The organic layers were separated and dried over anhydrous $MgSO_4$ to give **10b** (0.33 g, 67%) as brown oil. TLC $R_f = 0.38$ (EtOAc/*n*-hexane = 2:1); ^{1}H NMR (400 MHz, $CDCl_3$) δ 2.17 (t, $J = 2.4$ Hz, 1H, CC<u>H</u>), 2.86 (s, 3H, C<u>H</u>$_3$), 3.93 (dd, $J = 2.4$ Hz, 2H, C<u>H</u>$_2$CCH), 4.6 (s, 3H, C<u>H</u>$_2$), 6.69 (d, $J = 8.8$ Hz, 2H, aromatic <u>H</u>), 6.83 (d, $J = 8.8$ Hz, 2H, aromatic <u>H</u>), 7.18 (d, $J = 7.6$ Hz, 1H, aromatic <u>H</u>), 7.31 (d, $J = 8.4$ Hz, 1H, aromatic <u>H</u>), 7.42 (t, $J = 8$ Hz, 1H, aromatic <u>H</u>), 7.50 (d, $J = 8.8$ Hz, 1H, aromatic <u>H</u>), 8.1 (d, $J = 8.8$ Hz, 1H, aromatic <u>H</u>); ^{13}C-NMR (100 MHz, $CDCl_3$) δ 159.33, 155.09, 141.95, 141.69, 139.70, 136.82, 128.61, 126.32, 120.34, 119.69, 117.82, 114.29, 108.02, 79.62, 72.43, 51.25, 44.34, 39.64; IR (cm^{-1}): 3382.9, 1558.4, 1508.2; HRMS (EI): calcd. for $C_{21}H_{21}N_3O$ $[M]^+$, 331.1680; found, 331.1677.

Pharmacological evaluation

Thioflavin T assay

Preparation of the Aβ peptide: Aβ peptide (1–42) (Bachem Americas, CA, USA) was stored as a solid at −80°C. It was prepared to be stock peptide after removal from ice. 1,1,1,3,3,3-Hexafluoro-2-propanol (HFIP, Sigma–Aldrich, St. Louis, MO, USA) was on ice in the hood and used to dissolve Aβ peptide to give the final peptide concentration of 1 mM. The prepared stock solution was aliquotted to micro-centrifuge tubes and HFIP was removed by evaporation in the hood with traces removed under vacuum. All the tubes were then stored at −80°C and ready to be measured [34, 35].

Inhibition of metal-mediated Aβ aggregation: Each of aliquots of Aβ peptide in DMSO was diluted with phosphate buffer (50 mM, pH 7.4) to give 75 μM of the final Aβ (1–42) solution (DMSO <1%) before use. The resulting peptide solution (10 μL, 75 μM) treated with or without metal (10 μL, 75 μM $CuCl_2$ in HEPES buffer or 10 μL, 75 μM $ZnCl_2$ in HEPES buffer) was stood for 2 min followed by treating with the test compound (10 μL, 75 μM in HEPES buffer). The sample was incubated at 37°C for 24 h and subsequently treated with 50 mM glycine-NaOH buffer (pH 8.6) containing 5 μM ThT. Then 200 μL of the final sample was taken to 96-well microplate and measured with fluorescence intensities [36, 37].

Disaggregation of metal-triggered Aβ assembled fibrils: The peptide sample (10 μL, 75 μM) prepared with 10 μL, 75 μM $CuCl_2$ in HEPES buffer or 10 μL, 75 μM $ZnCl_2$ in HEPES buffer as above was incubated at 37°C for 24 h. The test compound (10 μL, 75 μM in HEPES buffer) was added and then incubated at 37°C for additional 24 h. After the sample was treated with 50 mM glycine-NaOH buffer (pH 8.6) containing 5 μM ThT, the final sample (200 μL) was taken to 96-well microplate and measured with fluorescence intensities [38, 39].

Transmission electron microscopy (TEM) assay

Preparation of samples for TEM assay were carried out according to the method reported previously [37, 40]. Glow-discharged grids (Formar/Carbon 300-mesh, Electron Microscopy Sciences) were treated with Aβ assembled samples (25 μM, 10 μL) for 5 min at room temperature. Excess samples were removed using filter paper and each grid was treated with 1% phosphotungstic acid (10 μL) for 2 min. After draining out excess staining solution, the resulting sample was taken for imaging by transmission electron microscope (JEOL JEM-1230).

Metal-chelating ability assay

The relative metal-chelating abilities of the modulator were examined by a UV–Vis spectrophotometer. The absorption spectra of the test compound (50 μM) alone or first in the presence of 50 μM of $CuCl_2$ or $ZnCl_2$ in methanol were recorded at room temperature. After the spectrum was first obtained, the resulting sample was followed by treating with the second metal (either $ZnCl_2$ or $CuCl_2$) as 50 μM in methanol solution and re-recorded to obtain the cumulative spectra. The final spectra could be evaluated on the relative metal-chelating properties of the test compound [41].

Inhibition of ROS by Amplex Red assay

The generation of H_2O_2 from an incubation of Cu^{2+} and ascorbate *in vitro* in a cell-free system was examined by using Amplex Red reagent as the detector in accordance with the reported method [26, 42]. Briefly, the test compound (10 μM) in 50 mM phosphate buffer (pH 7.4) was treated with Cu^{2+} ($CuCl_2$, 20 μM) and ascorbate (2 mM) and incubated at 37°C for 1 h along with 50 μM Amplex Red and 1 U/mL of HRP. A parallel group without the test compound was incubated with Cu^{2+} ($CuCl_2$, 20 μM) and ascorbate (2 mM), while another aliquot furnished with only 50 μM Amplex Red and 1 U/mL of HRP in buffer to be appropriate blank corrections was made. H_2O_2 reacts with Amplex Red in 1:1 stoichiometry in the presence of added horseradish peroxidase to generate resorufin, which was measured using a spectrofluorometer

set at λex (530 nm)/λem (590 nm) for recording the resulting absorbance.

Data analysis
The data presented as means ± SD from triplicates of each test compound treatment were measured in the experiments. The effects of the compound on the biological outcome were examined by using statistics of a one-way analysis of variance. Dunnet's test was applied to compare control to each of the other compound. In all cases, $P < 0.05$ was accepted to denote significance.

Authors' contributions

C.L. Fu and L.S. Hsu performed the synthesis of the designed compounds and parts of pharmacological experiments. Y.F. Liao conceived and designed the pharmacological experiments. M.K. Hu conceived and designed the targeted compounds and analyzed the data.

This work was supported by the grants from the Ministry of Science and Technology (former: National Science Council), Taiwan (NSC 98-2320-B-016-004-MY3 to M.K. Hu and NSC 98-2320-B-001-014-MY2 to Y.F. Liao). High-resolution mass spectra analyses performed by the Ministry of Science and Technology Regional Instruments Center at National Chiao Tung University are gratefully acknowledged.

The authors have declared no conflict of interest.

References

[1] J. Hardy, D. J. Selkoe, *Science* **2002**, *297*, 353–356.
[2] Z. S. Khachaturian, *Arch. Neurol*. **1985**, *42*, 1097–1105.
[3] T. Tomiyama, S. Matsuyama, H. Iso, T. Umeda, H. Takuma, K. Ohnishi, K. Ishibashi, R. Teraoka, N. Sakama, T. Yamashita, *J. Neurosci*. **2010**, *30*, 4845–4856.
[4] K. A. Vossel, K. Zhang, J. Brodbeck, A. C. Daub, P. Sharma, S. Finkbeiner, B. Cui, L. Mucke, *Science* **2010**, *330*, 198.
[5] M. Manto, *Toxics* **2014**, *2*, 327–345.
[6] A. Budimir, *Acta Pharm*. **2011**, *61*, 1–14.
[7] M. Cissé, F. Checler, *Neurobiol. Dis*. **2015**, *73*, 137–149.
[8] C. Chen, X. H. Li, Y. Tu, H. T. Sun, H. Q. Liang, S. X. Cheng, S. Zhang, *Neuroscience* **2014**, *257*, 1–10.
[9] F. Yu, P. Gong, Z. Hu, Y. Qiu, Y. Cui, X. Gao, H. Chen, J. Li, *J. Neuroinflammation* **2015**, *12*, 122–132.
[10] F. Mao, J. Yan, J. Li, X. Jia, H. Miao, Y. Sun, L. Huang, X. Li, *Org. Biomol. Chem*. **2014**, *12*, 5936–5944.
[11] A. K. Sharma, S. T. Pavlova, J. Kim, J. Kim, L. M. Mirica, *Metallomics* **2013**, *5*, 1529–1536.
[12] C. Kobylecki, T. Langheinrich, R. Hinz, E. R. Vardy, G. Brown, M. E. Martino, C. Haense, A. M. Richardson, A. Gerhard, J. M. Anton-Rodriguez, J. S. Snowden, D. Neary, M. J. Pontecorvo, K. Herholz, *J. Nucl. Med*. **2015**, *56*, 386–391.
[13] H. F. Kung, C. W. Lee, Z. P. Zhuang, M. P. Kung, C. Hou, K. Plössl, *J. Am. Chem. Soc*. **2001**, *123*, 12740–12741.
[14] P. J. Crouch, M. S. Savva, L. W. Hung, P. S. Donnelly, A. I. Mot, S. J. Parker, M. A. Greenough, I. Volitakis, P. A. Adlard, R. A. Cherny, C. L. Masters, A. I. Bush, K. J. Barnham, A. R. White, *J. Neurochem*. **2011**, *119*, 220–230.
[15] B. Bach, E. Haen, J. Marienhagen, G. Hajak, *Pharmacopsychiatry* **2005**, *38*, 178–179.
[16] R. Giacovazzi, I. Ciofini, L. Rao, C. Amatore, C. Adamo, *Phys. Chem. Chem. Phys*. **2014**, *16*, 10169–10174.
[17] H. Zhang, J. C. Rochet, L. A. Stanciu, *Biochem. Biophys. Res. Commun*. **2015**, *64*, 42–47.
[18] R. J. Ward, D. T. Dexter, R. R. Crichton, *J. Trace Elem. Med. Biol*. **2015**, *31*, 267–273.
[19] T. M. Ryan, B. R. Roberts, G. McColl, D. J. Hare, P. A. Doble, Q. X. Li, M. Lind, A. M. Roberts, H. D. Mertens, N. Kirby, C. L. Pham, M. G. Hinds, P. A. Adlard, K. J. Barnham, C. C. Curtain, C. L. Masters, *J. Neurosci*. **2015**, *35*, 2871–2884.
[20] A. K. Sharma, J. Kim, J. T. Prior, N. J. Hawco, N. P. Rath, J. Kim, L. M. Mirica, *Inorg. Chem*. **2014**, *53*, 11367–11376.
[21] M. Hassani, W. Cai, D. C. Holley, J. P. Lineswala, B. R. Maharjan, G. R. Ebrahimian, H. Seradj, M. G. Stocksdale, F. Mohammadi, C. C. Marvin, J. M. Gerdes, H. D. Beall, M. Behforouz, *J. Med. Chem*. **2005**, *48*, 7733–7749.
[22] E. Farkas, C. J. Sunman, *J. Org. Chem*. **1985**, *50*, 1110–1112.
[23] F. D. Bellamy, K. Ou, *Tetrahedron Lett*. **1984**, *25*, 839–842.
[24] C. A. Lipinski, F. Lombardo, B. W. Dominy, P. J. Feeney, *Adv. Drug Delivery Rev*. **1997**, *23*, 3–25.
[25] D. E. Clark, S. D. Pickett, *Drug Disc. Today* **2000**, *5*, 49–58.
[26] M. Sinha, P. Bhowmick, A. Banerjee, S. Chakrabarti, *Free Radic. Biol. Med*. **2013**, *56*, 184–192.
[27] D. Jiang, L. Men, J. Wang, Y. Zhang, S. Chickenyen, Y. Wang, F. Zhou, *Biochemistry* **2007**, *46*, 9270–9282.
[28] J.-S. Choi, J. J. Braymer, R. P. R. Nanga, A. Ramamoorthy, M. H. Lim, *Proc. Natl. Acad. Sci. U. S. A*. **2010**, *107*, 21990–21995.
[29] K. J. Barnham, E. C. L. Gautier, G. B. Kok, G. Krippner, **2004**, Patent WO2004007461 A1.
[30] G. Malecki, J. E. Nycz, E. Ryrych, L. Ponikiewski, M. Nowak, J. Kusz, J. Pikies, *J. Mol. Struct*. **2010**, *969*, 130–138.
[31] S. H. Chan, C. H. Chui, S. W. Chan, S. H. L. Kok, D. Chan, M. Y. T. Tsoi, P. H. M. Leung, A. K. Y. Lam, A. S. C. Chan, K. H. Lam, J. C. O. Tang, *ACS Med. Chem. Lett*. **2013**, *4*, 170–174.
[32] G.-P. Xue, P. B. Savage, K. E. Krakowiak, R. M. Izatt, J. S. Bradshaw, *J. Heterocyclic Chem*. **2001**, *38*, 1453–1457.

[33] Z. Li, E. Stankevicius, A. Ajami, G. Raciukaitis, W. Husinsky, A. Ovsianikov, J. Stampfl, R. Liska, *Chem. Commun*. **2013**, *49*, 7635–7637.
[34] T. Storr, M. Merkel, G. X. Song-Zhao, L. E. Scott, D. E. Green, M. L. Bowen, K. H. Thompson, B. O. Patrick, H. J. Schugar, C. Orvig, *J. Am. Chem. Soc*. **2007**, *129*, 7453–7463.
[35] C. Rodríguez-Rodríguez, N. S. de Groot, A. Rimola, A. Álvarez-Larena, V. Lloveras, J. Vidal-Gancedo, S. Ventura, J. Vendrell, M. Sodupe, P. González-Duarte, *J. Am. Chem. Soc* **2009**, *131*, 1436–1451.
[36] M. Groenning, L. Olsen, M. van de Weert, J. M. Flink, S. Frokjaer, F. S. Jørgensen, *J. Struct. Biol*. **2007**, *158*, 358–369.
[37] E. H. Nielsen, M. Nybo, S.-E. Svehag, *Methods Enzymol*. **1999**, *309*, 491–496.
[38] J. S. Choi, J. J. Braymer, R. P. Nanga, A. Ramamoorthy, M. H. Lim, *Proc. Natl. Acad. Sci. U. S. A*. **2010**, *107*, 21990–21995.
[39] C. Hureau, I. Sasaki, E. Gras, P. Faller, *ChemBioChem* **2010**, *11*, 950–953.
[40] C. G. Evans, S. Wisén, J. E. Gestwicki, *J. Biol. Chem*. **2006**, *281*, 33182–33191.
[41] A. K. Sharma, S. T. Pavlova, J. Kim, D. Finkelstein, N. J. Hawco, N. P. Rath, J. Kim, L. M. Mirica, *J. Am. Chem. Soc*. **2012**, *134*, 6625–6636.
[42] D. G. Smith, R. Cappai, K. J. Barnham, *Biochim. Biophys. Acta* **2007**, *1768*, 1976–1990.